Electrical Power and Energy Systems 115 (2020) 105462

Contents lists available at ScienceDirect

Electrical Power and Energy Systems

journal homepage: www.elsevier.com/locate/ijepes

Stability analysis of integrated power system with pulse load☆

Gang Wang, Runlong Xiao*, Chen Xu, Renji Huang, Xiaoliang Hao

National Key Laboratory of Science and Technology on Vessel Integrated Power System, Naval University of Engineering, No. 717 JieFang Avenue, Wuhan 430033, PR China

ARTICLE INFO

Keywords:
Integrated power system
Pulse load
Small-signal stability
Periodic orbit
State-space averaging method

ABSTRACT

The stability of an integrated power system (IPS) with pulse load involves both the trend of change in the system state during the whole period and the problem of whether to cause an unacceptable oscillation and an increase or decrease in the system state variable during a pulse period, which will pose a great challenge to the IPS. This paper considers the system stability in two aspects: the stability of system state variables in a periodic steady state under the action of pulse load, which refers to the stability of the periodic orbit, and the problem mentioned above, which cannot be described according to the stability of the equilibrium point and so needs further research. The analysis of the first aspect can lay the foundation for a study of the second aspect. This paper presents a mathematical model of the IPS with pulse load, uses the periodic-orbit method to analyze the system stability and stable margin and drives a state space averaging model of the system. For a relatively small state variable disturbance of the system under small signal disturbance, the state-space averaging method proves to be approximate to the periodic-orbit method. On this basis, the conventional state-space averaging method can be used for the analysis of system stability. The simulation and calculation show that the proposed method is feasible and effective.

1. Introduction

The pulse load means a periodic load with high power released in a very short time. Its pulse period is a couple of seconds. The released power ranges from several hundred kilowatts to several megawatts, as is the case for radar, laser beam weapon, electromagnetic rail gun and launcher [1,2]. The pulse load releases pulse energy intermittently, with quite high energy density and power density and is usually powered by energy storage devices [3,4]. In a traditional mechanically-propelled ship, most of its output of the power system is used to drive the propulsion device by mechanical energy, and the remaining part supplies electricity to the daily service loads through electrical energy. Even if a mechanically-propelled ship is equipped with the energy storage system, the operation of pulse load is difficult to guarantee.

The integrated power system (IPS) is a big leap in the field of modern ship power systems, marking the future direction of development. It combines the dynamic system and the power system which are independent of each other and provides the loads with electrical energy, which is prerequisite for the application of pulse load and also an only road to the development of a ship platform from mechanization to electrification and informatization [5–7]. The intermittent impact of the pulse load on the power system differs from the disturbance caused by abrupt change of loads in the traditional power system, in that it is characterized by high-energy density, high-power density and periodicity, which brings a tremendous challenge to the power system in terms of transient performance, stability and power quality [8,9].

The small-signal stability for IPS refers to whether the system will be able to maintain synchronism when it has been subjected to small disturbances due to abrupt load change, motor start-up, pulse load in use and so on [10]. Because small disturbances are difficult to avoid, the IPS cannot operate normally in practical conditions if the system is unstable. For this reason, judging whether the IPS has small-signal stability in its specified operation is a very important task in the analysis and design of IPS. As for the periodical charge-and-discharge process of the pulse load, the IPS does not have a mere equilibrium point, it includes a periodic alternating process of system variables. The periodic orbit can be used to represent the steady-state operation of the system. The dynamic response characteristics of IPS can be expressed by differential equations. $\boldsymbol{x}_0$ is the initial value, the solution of the differential equation will return to $\boldsymbol{x}_0$ after a period of time. Then the solution during this time is called the periodic orbit of the equation. On entering the periodic orbit the state variables will constantly stay on it. Similar to Lyapunov stability definition for equilibrium point, the orbital asymptotic stability of the periodic orbit means that the solution of

☆ This work was financially supported by National Key Basic Research Program 973 Project of China (613294).
* Corresponding author.
E-mail address: runlxiao@foxmail.com (R. Xiao).

https://doi.org/10.1016/j.ijepes.2019.105462
Received 22 February 2019; Received in revised form 18 June 2019; Accepted 1 August 2019

the differential equation starting from any point near the periodic orbit is still nearby, and the difference between the solution and the periodic orbit tends to zero as time approaches the infinity [11,12].

The stability of IPS with pulse load refers to two aspects. The first aspect is about the stability of system variables in periodic steady state under the action of pulse load. The action of the pulse load on the system is generally considered with the pulse duration as a unit, which merely involves the changing trend of sampled state variables in the pulse duration but not changes in state variables in one pulse period. This can be investigated either by the system periodic-orbit stability method, or by the state-space averaging method with which to transform the periodic orbit stability into the equilibrium point stability after simplification [13,14]. The second aspect is about whether there is an unacceptable oscillation, increase or decrease in the state variable during a pulse period. As the steady state of state variables is not the equilibrium point at this time, this phenomenon cannot be described according to the stability of equilibrium point. And its methods for the definitions and analysis of stability need to be further studied. Considering the first aspect is prerequisite for the second aspect in the analysis or study of stability, this paper first makes a study of the system periodic-orbit stability so as to lay the foundation for researching the second aspect of the system stability.

Related researches on the stability of the IPS with pulse load mainly refer to specific disturbances, and the use of time-domain simulation method [15] and Hamilton surface-forming method [16] for studying the system stability. As for the time-domain simulation method, its disturbance and observational variables have a great influence on the result. Because of lack of credibility and too much time spent on the time-domain calculation, the method is not suitable for the analysis of stability in the stage of system design. Moreover, due to its unclear physical concept, it is difficult to directly find out the cause of system instability through the simulation results. Therefore, corresponding measurements of improvement are needed. The stability analysis of small-signal disturbance is based on Floquet theory of periodic orbit, this method is only suitable for a time-variant linear system. However, the system in Ref. [16] is not a strictly linear system because its state Eq. (2) contains the item of $P(t)/v_C$, so the method is an approximate one. The use of Hamilton surface-forming method to establish energy function for an ordinary system is difficult. Neither of these two methods is applicable to distinguishing between the two aspects concerning the system stability, so it is necessary to find a method for analyzing the first aspect of system stability based on periodic orbit stability. Ref. [17] did not refer to the stability analysis of small-signal disturbance but to the algorithm of periodic steady-state performance of the IPS with pulse load. The algorithm means solving for the periodic orbit to assess the power quality of the system.

This paper includes the following sections. Section 2 describes the state-space averaging method and the periodic-orbit method for system stability. Section 3 refers to the relationship between these two methods. Section 4 is about the simulation and verification of the proposed methods. Section 5 gives a conclusion.

2. Stability analysis on IPS with pulse load

2.1. Periodic-orbit method

As the pulse load has high power in a short time, it makes strict demands on the vessel power system. This paper deals with the operational characteristics of the pulse load, as shown in Fig. 1. Fig. 1(a) shows the rectangular-wave pulse load, whose charge-and-discharge curves display discontinuous features [18]. As for its parameters, $\boldsymbol{T}$ denotes the pulse period, $\boldsymbol{D}$ the duty cycle, $\boldsymbol{P}_1$ the low-value power and $\boldsymbol{P}_2$ the high-value power. Fig. 1(b) shows the triangular-wave pulse load, whose charge-and-discharge process curves display continuous features [19]. $\boldsymbol{T}$, $\boldsymbol{P}_1$ and $\boldsymbol{P}_2$ represent the pulse period, low-value power and high-value power, respectively.

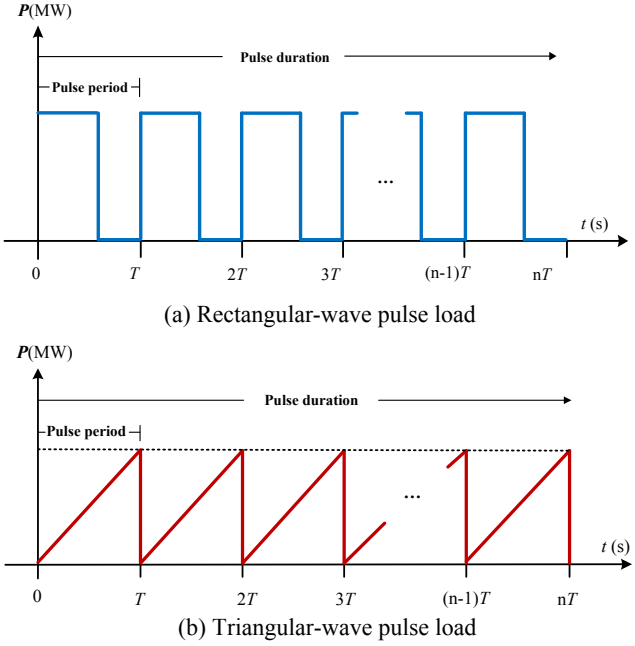

Fig. 1. Operational characteristics of pulse load.

The dynamic response of IPS with the pulse load can be expressed as:

$$\frac{d\boldsymbol{x}}{dt} = \boldsymbol{f}(\boldsymbol{x}, t) \tag{1}$$

where the state variable $\boldsymbol{x}$ is a m-dimension vector and $\boldsymbol{f}(\boldsymbol{x})$ is a function of $\boldsymbol{T}$, that is, $\boldsymbol{f}(\boldsymbol{x},t+\boldsymbol{T}) = \boldsymbol{f}(\boldsymbol{x},t)$.

The system equation contains a function of $\boldsymbol{T}$ due to the application of the pulse load. At this time, the system steady state is the periodic orbit. There are two methods to calculate the periodic orbit, namely the time-domain simulation method and the analytic method. The time-domain simulation method deals with specific disturbances by use of numerical calculation of the differential equation to get a complete time-domain response of state variables. After a very long time in simulation, the system enters a periodic steady state, which indicates the periodic orbit is acquired. However, the method has some disadvantages, such as time-consuming calculation, unclear physical concepts and difficulty in using the simulation results to quantitatively evaluate the factors affecting the periodic orbit. The analytic method is adopted to formulate equations which are used to calculate the periodic orbit. The quick calculation characteristic of the method makes it possible to evaluate the factors influencing the periodic orbit quantitatively through the sensitivity analysis [17].

The analytic method for calculating the periodic orbit is given below. The period $\boldsymbol{T}$ is divided into n parts, with n taken as 100 generally; the discretized time step is $\boldsymbol{h} = \boldsymbol{T}/n$; the time points are $t_0, t_1, \cdots, t_n$ respectively, among which $t_i = ih$; the state variables are $\boldsymbol{x}_0,\boldsymbol{x}_1,\ldots\boldsymbol{x}_n$ respectively. The use of the implicit trapezoidal integral method leads to the formulation of equations for periodic orbit as follows:

$$\begin{aligned} \boldsymbol{x}_{i-1} + \tfrac{h}{2}[\boldsymbol{f}(\boldsymbol{x}_{i-1}, t_{i-1}) + \boldsymbol{f}(\boldsymbol{x}_i, t_i)] - \boldsymbol{x}_i = 0 \quad i = 1, \cdots, n \quad (2-1) \\ \boldsymbol{x}_n - \boldsymbol{x}_0 = 0 \qquad\qquad (2-2) \end{aligned} \tag{2}$$

where Eq. (2-1) is the implicit trapezoidal integral formula and Eq. (2-2) represents the terms satisfying the periodic orbit.

The Newton-Raphson method is used to solve the above equations for the system periodic obit and their initial value is obtained by the state-space averaging method. And the Newton-Raphson method is a solution to the non-linear equations of second-order convergence.

Because of rapid convergence, a few iterations are generally needed to get the solutions $\boldsymbol{x}_{0e}, \boldsymbol{x}_{1e}, \cdots, \boldsymbol{x}_{ne}$. If the scale of the system is quite large and the pulse period is relatively long, the periodic-orbit method will have to do much more computation than the time-domain simulation method. Therefore, it is necessary to investigate a fast algorithm for the periodic orbit. Using the time-domain simulation method as a reference, this paper proposes a periodic-orbit method based on sensitivity analysis. According to Eq. (2-1), given the initial variable $\boldsymbol{x}_0$, it follows that the next variable is $\boldsymbol{x}_1$. Then the variable $\boldsymbol{x}_n$ can be obtained from successive recursion. That is a process of calculating the state variables in one period by the time-domain simulation method. If several periods are repeatedly calculated until the norm of difference between $\boldsymbol{x}_0$ and $\boldsymbol{x}_n$ is sufficiently small, the periodic orbit can be obtained with the time-domain simulation method. The method needs large computation because it passively waits for the system to enter a periodic steady state. It is worthy of note that the Poincaré mapping of the periodic orbit is defined in Eq. (2-1). To compute its Jacobian matrix, the partial differential calculation of the previous state variable $\boldsymbol{x}_{i-1}$ in accordance to $\boldsymbol{x}_i$ in Eq. (2-1) can lead to:

$$\frac{\partial \boldsymbol{x}_i}{\partial \boldsymbol{x}_{i-1}} = \left(\boldsymbol{I} - \frac{h}{2}\boldsymbol{A}_i\right)^{-1}\left(\boldsymbol{I} + \frac{h}{2}\boldsymbol{A}_{i-1}\right) \qquad i = 1, \cdots, n \tag{3}$$

where $\boldsymbol{A}_i = \left.\frac{\partial f}{\partial \boldsymbol{x}_i}\right|_{(\boldsymbol{x}_{ie}, t_i)}$, $\boldsymbol{I}$ is the m-dimension unit matrix.

Jacobian matrix of Poincaré mapping, or the $\boldsymbol{x}_n$-$\boldsymbol{x}_0$ sensitivity matrix at the periodic orbit $\boldsymbol{x}_{0e}, \boldsymbol{x}_{1e}, \cdots, \boldsymbol{x}_{ne}$ is:

$$\boldsymbol{M} = \frac{\partial \boldsymbol{x}_n}{\partial \boldsymbol{x}_0} = \prod_{i=1}^{n}\left(\boldsymbol{I} - \frac{h}{2}\boldsymbol{A}_i\right)^{-1}\left(\boldsymbol{I} + \frac{h}{2}\boldsymbol{A}_{i-1}\right) \tag{4}$$

If the matrix multiplication does not meet the commutative law, the above equation needs to be calculated in turn.

Supposing the disturbance Δx_0 is added to $\boldsymbol{x}_0$, the disturbance Δx_n will be added to $\boldsymbol{x}_n$ accordingly. By the linear approximation, Δx_n is expressed as

$$\Delta \boldsymbol{x}_n = \boldsymbol{M}\Delta \boldsymbol{x}_0 \tag{5}$$

To make the sum of $\boldsymbol{x}_0$ and Δx_0 equal to that of $\boldsymbol{x}_n$ and Δx_n, the disturbance Δx_0 should be taken from the following equation:

$$\Delta \boldsymbol{x}_0 = (\boldsymbol{I} - \boldsymbol{M})^{-1}(\boldsymbol{x}_n - \boldsymbol{x}_0) \tag{6}$$

In the strict sense, the sum of $\boldsymbol{x}_0$ and $\Delta \boldsymbol{x}_0$ is not equal to that of $\boldsymbol{x}_n$ and $\Delta \boldsymbol{x}_n$ due to an error in linearization. But with the error converging to zero gradually and its norm becoming small enough, the periodic orbit can be obtained.

To make the system operate stably, the spectral radius of Jacobian matrix of Poincaré mapping of the periodic orbit (the maximum modulus of its eigenvalue) must be less than 1. With $\rho(\boldsymbol{M})$ as the spectral radius of $\boldsymbol{M}$, the stable margin is expressed by the difference between 1 and $\rho(\boldsymbol{M})$.

$$\boldsymbol{S}_m = 1 - \rho(\boldsymbol{M}) \tag{7}$$

According to the theory of periodic orbit stability of the nonlinear dynamic system, if $\boldsymbol{S}_m > 0$, the system is stable, and the larger its value, the more stable the system; if $\boldsymbol{S}_m < 0$, the system is unstable.

2.2. State-Space averaging method

Because of the periodicity of function $\boldsymbol{f}(\boldsymbol{x},t)$, on the right side of Eq. (1) is a time-varying variable. For this reason, the period T is divided into n parts, where n is big enough to make the right side of Eq. (1) approximate to a constant. Then the piecewise equation is:

$$\frac{d\boldsymbol{x}}{dt} = \boldsymbol{f}(\boldsymbol{x}, t) \qquad t \in [\, t_{i-1}, \ t_i] \qquad i = 1, \cdots, n \tag{8}$$

where there are n segments and the duty cycle of each segment is $1/n$. The averaging of the state space in $\boldsymbol{T}$ leads to:

$$\frac{d\boldsymbol{x}}{dt} = \boldsymbol{g}(\boldsymbol{x}) = \frac{\int_0^T \boldsymbol{f}(\boldsymbol{x}, t)dt}{\boldsymbol{T}} \tag{9}$$

Here, $\boldsymbol{g}(\boldsymbol{x})$ is the average function of state-space of $\boldsymbol{f}(\boldsymbol{x})$, and uses the average value instead of the characteristic of pulse load so as to eliminate the periodicity of system differential equation and transform the stability of periodic orbit into that of equilibrium point.

The equilibrium point $\boldsymbol{x}_e$ and its characteristic matrix $\boldsymbol{A}_e$ are respectively expressed as:

$$\begin{aligned} &\boldsymbol{g}(\boldsymbol{x}_e) = 0 \\ &\boldsymbol{A}_e = \left.\frac{\partial \boldsymbol{g}}{\partial \boldsymbol{x}}\right|_{\boldsymbol{x}_e} \end{aligned} \tag{10}$$

If all the eigenvalues of $\boldsymbol{A}_e$ contain the negative real parts, the system is stable. If the eigenvalues of $\boldsymbol{A}_e$ contain the positive real parts, the system is unstable.

The state-space averaging method aims at turning the stability of periodic orbit into that of equilibrium point. Although it can be used for stability analysis approximately, the method is characterized by simpler modeling, less calculation and clearer physical concepts.

In Ref. [13], the state-space averaging method was applied to the linear system, proving that the time-domain solution of its state variables in one pulse period is linearly approximate to its exact solution in the modulation period, that is, the difference between the two only includes the quadratic term and the maximum term in the modulation period. For the non-linear system, the linearizing method can be adopted to make it approximate to the linear system. As the modulation period is very short when the traditional state-space averaging method is used, the method is approximately reasonable. The derivation process from (8) to (9) differs from that by the traditional state-space averaging method because $\boldsymbol{T}$ counted generally as several seconds is relatively large and the system equation is non-linear. The traditional linear equation or non-linear equation derivation method is no longer applicable, which indicates that (8) and (9) are merely regarded as extrapolations of the state-space averaging method, whose applicability needs to be studied.

3. Relationship between two stability analysis methods

From above analysis, it is known that the periodic-orbit method is a strict approach to analyzing the stability of the system with pulse load, and that the state-space averaging method is an approximate one and its approximate conditions cannot satisfy the stability analysis, so it is made extrapolative. The applicability of state-space averaging method needs to be studied. This section describes the applicability of the state-space averaging method based on the periodic-orbit method.

When h is sufficiently small, the equations obtained according to matrix multiplication are as following:

$$\left(\sum_{j=0}^{\infty}\left(\frac{h}{2}\boldsymbol{A}_i\right)^j\right)\left(\boldsymbol{I} - \frac{h}{2}\boldsymbol{A}_i\right) = \left(\boldsymbol{I} - \frac{h}{2}\boldsymbol{A}_i\right)\left(\sum_{j=0}^{\infty}\left(\frac{h}{2}\boldsymbol{A}_i\right)^j\right) = \boldsymbol{I} \qquad i = 1, \cdots, n \tag{11}$$

The combination of (4) with (11) leads to:

$$\boldsymbol{M} = \prod_{i=1}^{n}\left(\sum_{j=0}^{\infty}\left(\frac{h}{2}\boldsymbol{A}_i\right)^j\right)\left(\boldsymbol{I} + \frac{h}{2}\boldsymbol{A}_{i-1}\right) \tag{12}$$

For the small-signal stability of the system, the disturbance of the state variable is relatively small, and the system with pulse load needs to meet the corresponding standards of its voltage and frequency, for example, the voltage variation must be less than 2% of the rated value when the pulse load is applied [3]. On this basis, the state variable slightly fluctuating near the rated value can be extrapolated when the pulse load is applied. The equation is assumed to be

$$\boldsymbol{A}_i = \boldsymbol{A}_j = \boldsymbol{A}_e \qquad i, j = 1, \cdots, n \tag{13}$$

When the state matrixes $\boldsymbol{A}_i$ and $\boldsymbol{A}_j$ can be exchanged, the state-space averaging method is of higher accuracy [13]. Because $\boldsymbol{A}_i$ and $\boldsymbol{A}_j$ in this paper do not involve the switching of the system topology but fluctuations in the state variables caused by a fluctuation in pulse load, they are considered approximately equal. This assumption is reasonable and will be further verified by the following numerical examples.

According to the above assumption and the matrix exponential function defined as $e^{\boldsymbol{A}} = \sum_{j=0}^{\infty} \frac{\boldsymbol{A}^j}{j!}$, the expansion of each factor in (12) into a cubic term leads to:

$$\boldsymbol{M} = \prod_{i=1}^{n} \left(e^{\boldsymbol{A}_e h} + \boldsymbol{O}(h^3)\right) \tag{14}$$

where $\boldsymbol{O}(h^3)$ is the infinitesimal of h^3 in the same order.

$\boldsymbol{O}(h^3)$ contains n terms in addition to $\prod_{i=1}^{n} e^{\boldsymbol{A}_e h}$, so the following expression is:

$$\boldsymbol{M} = e^{\boldsymbol{A}_e T} + \boldsymbol{O}(h^2) \tag{15}$$

where $e^{\boldsymbol{A}_e T}$ is a satisfactory approximation of $\boldsymbol{M}$ in the sense of small-signal stability.

According to the matrix theory, if all the eigenvalues of $\boldsymbol{A}_e$ contain negative real parts, the spectral radius of $\boldsymbol{M}$ matrix is less than 1; if all the eigenvalues of $\boldsymbol{A}_e$ contain positive real parts, the spectral radius of $\boldsymbol{M}$ is greater than 1. Therefore, the state-space averaging method is equivalent to the periodic-orbit method for the stability analysis of the system with pulse load. Thus, the traditional state-space averaging method can be used for that purpose.

4. Simulation of system stability

The case shown in Fig. 2 is taken for example, which is similar to the system shown in Fig. 2 of Ref. [16]. The study is focused on the stability of the system with periodic pulse load. The case is relatively simple, but it can concisely display the effectiveness of the periodic-orbit method and the state-space averaging method with which to deal with the problem of system stability. The parameters are listed in Table 1. The voltage of the bus bar is DC1KV, the total daily service loads are $\boldsymbol{R} = 2\,\Omega$, and the combination of propulsion load $\boldsymbol{P}_0$ with the pulse load is represented by the constant power load $\boldsymbol{P}$. $\boldsymbol{T}$ is the pulse period, $\boldsymbol{P}_1$ and $\boldsymbol{P}_2$ are respectively the low- and high-value power, $\boldsymbol{D}$ is the duty cycle (only suitable for the rectangular-wave pulse load). The data in Table 1 is known as reference data.

The system differential equations are as follows:

$$\begin{aligned} \frac{d\boldsymbol{i}_L}{dt} &= -\frac{\boldsymbol{R}_1}{\boldsymbol{L}}\boldsymbol{i}_L - \frac{\boldsymbol{R}_1}{\boldsymbol{L}}\boldsymbol{u}_c + \frac{\boldsymbol{V}}{\boldsymbol{L}} \\ \frac{d\boldsymbol{u}_c}{dt} &= \frac{1}{\boldsymbol{C}}\boldsymbol{i}_L - \frac{1}{\boldsymbol{CR}}\boldsymbol{u}_c - \frac{\boldsymbol{P}}{\boldsymbol{C}\boldsymbol{u}_c} \end{aligned} \tag{16}$$

where $\boldsymbol{i}_L$, $\boldsymbol{u}_c$ and $\boldsymbol{P}$ denote the inductance current, capacitance voltage and load power, respectively.

During the period of 40 s, the total load is $\boldsymbol{R} = 2\,\Omega$, the propulsion load is $\boldsymbol{P}_0 = 1.6$ MW, $\boldsymbol{P}_1$ and $\boldsymbol{P}_2$ are respectively the low- and high-value power of the pulse load, and $\boldsymbol{P}_1 = 0$, $\boldsymbol{P}_2 = 0.4$ MW. At this time, the system is stable and goes into a steady state at 40 s, at which the high-value power $\boldsymbol{P}_2$ of the pulse load suddenly rises from 0.4 MW to 0.55 MW and 0.62 MW, respectively, whose time-domain response

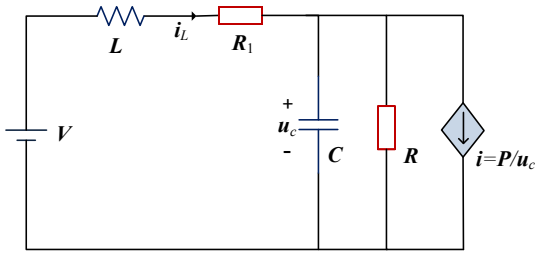

Fig. 2. The system with pulse load.

Table 1
Parameters of ips.

$\boldsymbol{V}$	$\boldsymbol{L}$	$\boldsymbol{R}_1$	$\boldsymbol{C}$	$\boldsymbol{R}$
1000 V	2mH	0.01 Ω	0.3F	2 Ω
$\boldsymbol{P}_0$	$\boldsymbol{T}$	$\boldsymbol{P}_1$	$\boldsymbol{P}_2$	$\boldsymbol{D}$
1.6 MW	4 s	0 MW	0.4 MW	50%

curves of state variables are shown in Figs. 3 and 4 respectively. In the calculation n is taken as 400, the lower portion of each figure (marked with *) shows a changing tendency in the case of taking the value of state variable only at the beginning of each period. Under the condition of rectangular-wave pulse or triangular-wave pulse, the periodic orbit is stable when $\boldsymbol{P}_2$ increases to 0.55 MW, and it is unstable when $\boldsymbol{P}_2$ rises to 0.62 MW. In each pulse period, the state variable oscillates attenuatively due to low-value power pulse and incrementally due to high-value power pulse. Figs. 3 and 4 indicate that the critical stable high-value power of pulse load is between 0.55 MW and 0.62 MW.

The state-space averaging model of the system is expressed as:

$$\begin{aligned} \frac{d\bar{\boldsymbol{i}}_L}{dt} &= -\frac{\boldsymbol{R}_1}{\boldsymbol{L}}\bar{\boldsymbol{i}}_L - \frac{\boldsymbol{R}_1}{\boldsymbol{L}}\bar{\boldsymbol{u}}_c + \frac{\boldsymbol{V}}{\boldsymbol{L}} \\ \frac{d\bar{\boldsymbol{u}}_c}{dt} &= \frac{1}{\boldsymbol{C}}\bar{\boldsymbol{i}}_L - \frac{1}{\boldsymbol{CR}}\bar{\boldsymbol{u}}_c - \frac{\boldsymbol{P}_e}{\boldsymbol{C}\bar{\boldsymbol{u}}_c} \end{aligned} \tag{17}$$

where $\bar{\boldsymbol{i}}_L$ and $\bar{\boldsymbol{u}}_c$ represent the average value of state space in a pulse period, and $\boldsymbol{P}_e = \boldsymbol{P}_0 + (\boldsymbol{P}_1 + \boldsymbol{P}_2)/2$ is the equivalent average power of $\boldsymbol{P}$. As there is not much change in capacitor voltage $\boldsymbol{u}_c$, here is the assumption: $\int_0^T \frac{\boldsymbol{P}}{\boldsymbol{u}_c} dt = \frac{\boldsymbol{P}_0 + (\boldsymbol{P}_1 + \boldsymbol{P}_2)/2}{\boldsymbol{C}\bar{\boldsymbol{u}}_c}$。

Considering $\boldsymbol{R}_1$ is relatively small, the periodic-orbit method and the state-space averaging method are used to calculate the critical stable high-value power of the pulse load; as shown in Table 2, the system equilibrium point approaches that value and thus is expressed as:

$$\bar{\boldsymbol{u}}_{c0} = \boldsymbol{V}\left(1 - \frac{\boldsymbol{R}_1}{\boldsymbol{R}} - \frac{\boldsymbol{R}_1\boldsymbol{P}_e}{\boldsymbol{V}^2}\right) \quad \bar{\boldsymbol{i}}_{L0} = \frac{\boldsymbol{V}}{\boldsymbol{R}} + \frac{\boldsymbol{P}_e}{\boldsymbol{V}} \tag{18}$$

The critical value of equivalent average power is approximate to

$$\boldsymbol{P}_{ec} = \frac{\boldsymbol{V}^2(1 - 2\boldsymbol{R}_1/\boldsymbol{R})}{2\boldsymbol{R}_1 + 1/(1/\boldsymbol{R} + \boldsymbol{R}_1\boldsymbol{C}/\boldsymbol{L})} \tag{19}$$

Then, the approximate critical value of equivalent power is

$$\boldsymbol{P}_{2c} = 2(\boldsymbol{P}_{ec} - \boldsymbol{P}_0) - \boldsymbol{P}_1 \tag{20}$$

$\boldsymbol{P}_2$ of the pulse load is continuously increased until the spectral radius of Jacobian matrix of Poincaré mapping of the periodic orbit is up to 1, then the critical stable $\boldsymbol{P}_2$ is obtained by the periodic-orbit method. The calculation of $\boldsymbol{P}_2$ by the state-space averaging method is shown in (19) and (20), as well as in Table 2. Obviously the result obtained from calculation by the state-space averaging method is very close to that by the periodic-orbit method, which is in agreement with the critical stable high-value power of the pulse load that is between 0.55 MW and 0.62 MW, shown in Figs. 3 and 4. When the change of n in adopting the periodic-orbit method has no influence on the critical stability.

With n taken as 4000 and $\boldsymbol{P}_2$ increased continuously, the spectral radius of Jacobian matrix $\boldsymbol{M}$ changes, as shown in Table 3 and Fig. 5. The solid lines represent the results of the triangular-wave pulse load, while the dotted lines represent the results of the rectangular-wave pulse load. By comparison, the rectangular-wave pulse load easily loses stability because it experiences power step twice in one pulse period. However, the triangular-wave pulse load experiences power step only once in a pulse period. The values of power step of both the pulse loads are equal in comparison.

In the use of reference data and variation data, the later is only utilized to adjust the high-value power of the pulse load to critical value. By taking n as 1000, the periodic orbit is calculated, as shown in Fig. 6, where the dotted line and the solid line correspond to the reference data and the variation data, respectively; the operating points in the use of the

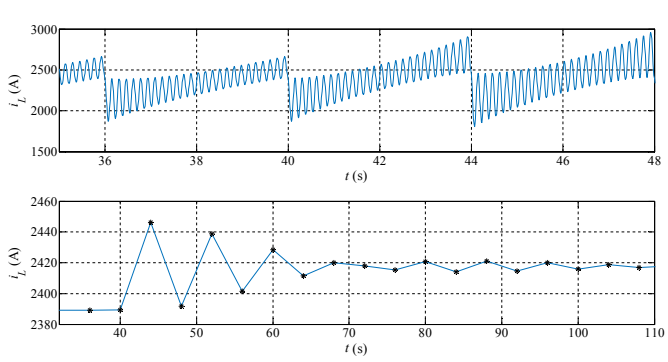

(a) Inductance current under triangular-wave pulse load

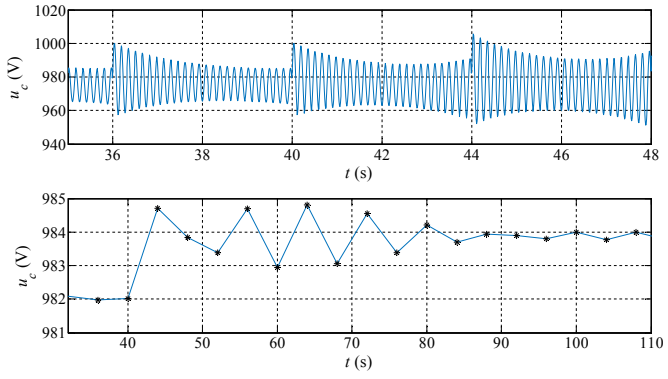

(b) Capacitance voltage under triangular-wave pulse

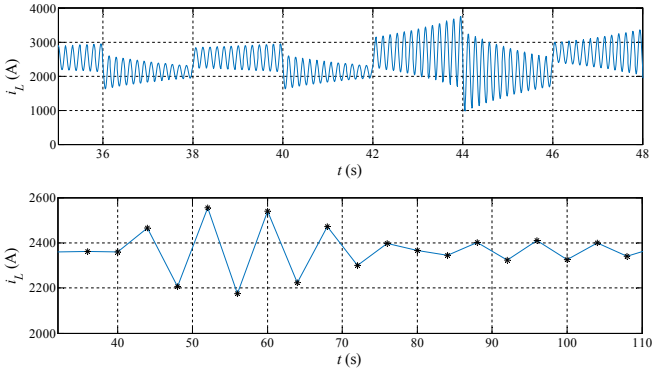

(c) Inductance current under rectangular-wave pulse load

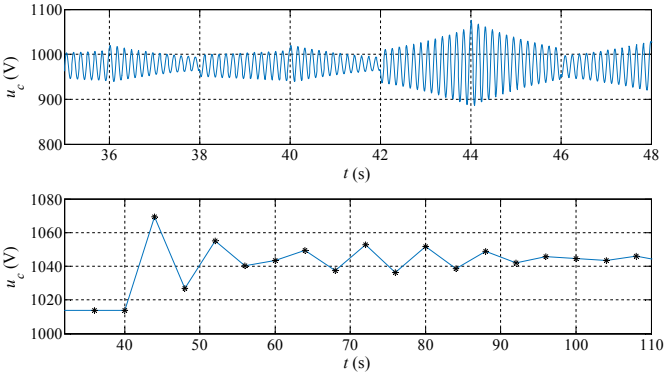

(d) Capacitance voltage under rectangular-wave pulse load

Fig. 3. Response curves of state variable with P_2 increasing to 0.55 MW.

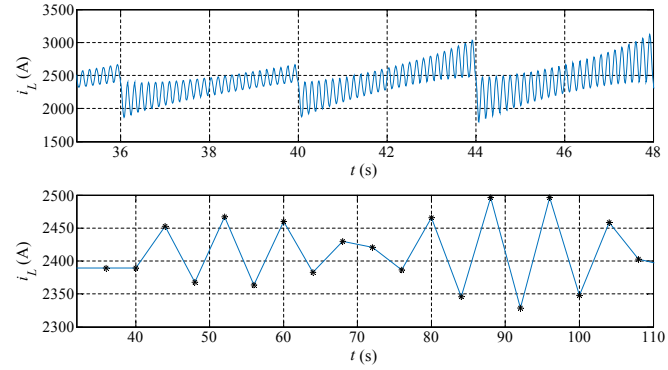

(a) Inductance current under triangular-wave pulse load

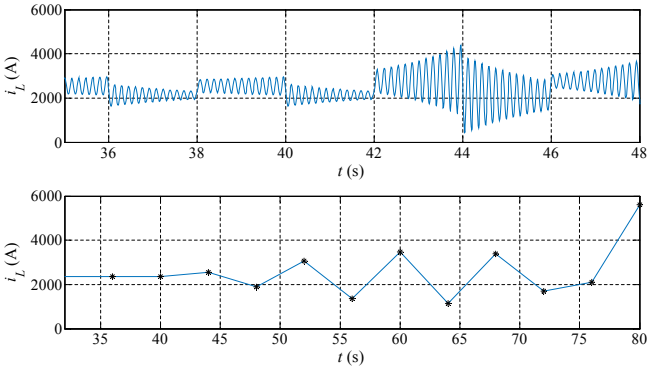

(c) Inductance current under rectangular-wave pulse load

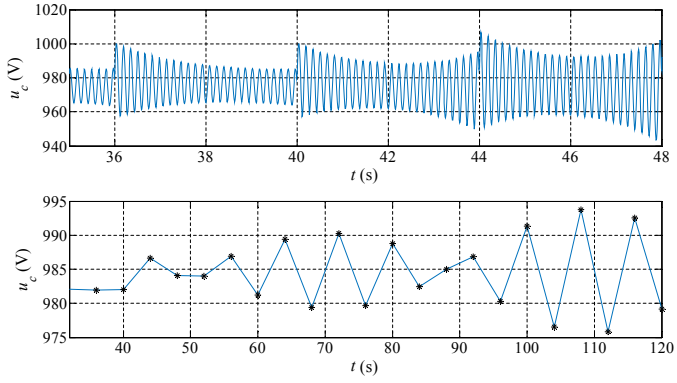

(b) Capacitance voltage under triangular-wave pulse load

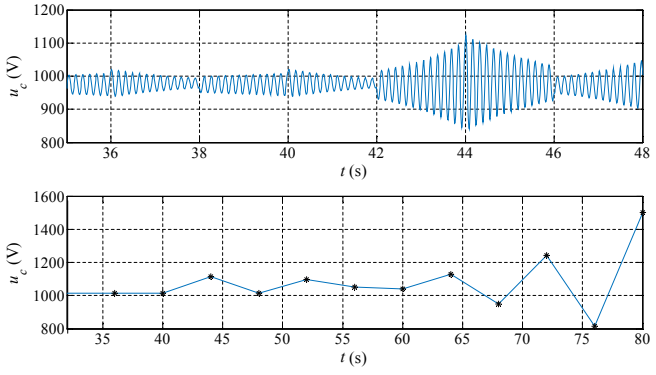

(d) Capacitance voltage under rectangular-wave pulse load

Fig. 4. Response curves of state variable with P_2 increasing to 0.62 MW.

Table 2
Critical stable high-value power of pulse load.

Method	Pulse load	n = 400	n = 1000	n = 2000	n = 4000
The periodic-orbit method	Triangular-wave	0.60 MW	0.60 MW	0.60 MW	0.60 MW
	Rectangular-wave	0.59 MW	0.59 MW	0.59 MW	0.58 MW
The state-space averaging method	Both	0.61 MW			

Table 3
Critical stable high-value power of the pulse load.

P_2(MW)	0.40	0.50	0.54	0.56	0.58
Triangular-wave Pulse	0.4759	0.6887	0.7986	0.8599	0.9259
Rectangular-wave Pulse	0.4811	0.7100	0.8341	0.9050	0.9826
P_2(MW)	0.59	0.60	0.61	0.62	
Triangular-wave Pulse	0.9608	0.9970	1.035	1.073	
Rectangular-wave Pulse	1.024	1.068	1.113	1.160	

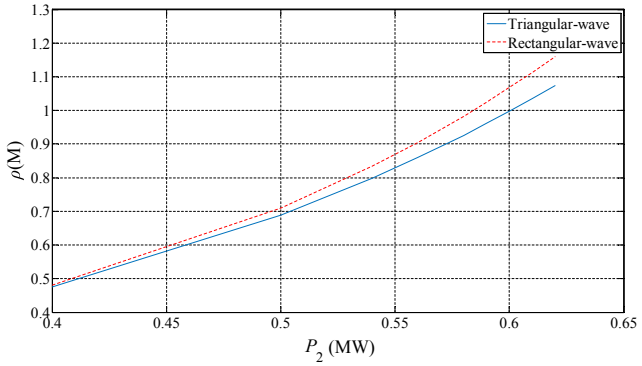

Fig. 5. Relationship between ρ(***M***) and P_2 in using periodic-orbit method.

state-space averaging method are [2300 A, 977 V] and [2400 A, 976 V], respectively. It is obvious that the periodic orbit oscillates near the operating point without much difference. There is a bigger fluctuation in the periodic orbit of rectangular-wave pulse than in the periodic orbit of triangular-wave pulse under the same load. With an increase in the load, the periodic orbit fluctuates more greatly. Fig. 6(a) shows the periodic orbit of the system in the use of reference data and variation data, and the system is stable or critical stable, respectively. The difference in magnitude increases with time because the oscillation in magnitude of the system in the use of variation data is bigger than the oscillation in magnitude of the system in the use of reference data.

The Jacobian matrix $\boldsymbol{M}$ is calculated by use of Eq. (4), and $\boldsymbol{A}_i$ is expressed as:

$$\boldsymbol{A}_i = \begin{bmatrix} -\frac{R_1}{L} & -\frac{1}{L} \\ \frac{1}{C} & -\frac{1}{CR} + \frac{P_i}{Cu_{ci}^2} \end{bmatrix} \tag{21}$$

where $\boldsymbol{P}_i$ and $\boldsymbol{u}_{ci}$ denote the load power and the periodic-orbit capacitance voltage at the ith moment, respectively.

According to Eq. (10), Matrix $e^{\boldsymbol{A}_e T}$ is calculated with the state-space averaging method, $\boldsymbol{A}_e$ is expressed as:

$$\boldsymbol{A}_e = \begin{bmatrix} -\frac{R_1}{L} & -\frac{1}{L} \\ \frac{1}{C} & -\frac{1}{CR} + \frac{P_e}{C\bar{u}_{c0}^2} \end{bmatrix} \tag{22}$$

With $\boldsymbol{M}$ as a criterion, the relative error in the norm between $\boldsymbol{M}$ and $e^{\boldsymbol{A}_e T}$ is compared. As shown in Table 4, the error is small. The Comparison of the rectangular-wave pulse with the triangular-wave pulse under the same load indicate that there is a bigger error in the norm between the two matrixes. Furthermore, the error increases with the load, and it becomes small as n increases.

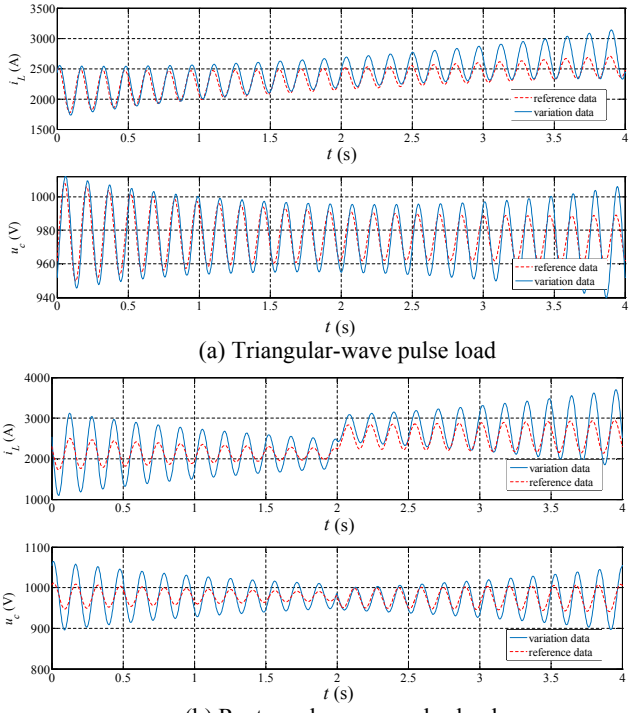

(a) Triangular-wave pulse load

(b) Rectangular-wave pulse load

Fig. 6. The periodic orbit of the system.

With $\boldsymbol{M}$ as the standard, the relative error in spectral radius between $\boldsymbol{M}$ and $e^{\boldsymbol{A}_e T}$ is found to be small through comparison, as shown in Table 5. The comparison of the rectangular-wave pulse with the triangular-wave pulse under the same load shows that the error between the two matrixes is bigger. With an increase in the load, the error becomes large, and it becomes small as n increases. A comparatively big error appearing in the variation data is due to a large fluctuation in voltage at this time.

Table 4
The relative error in the norm between matrixes M and $e^{\boldsymbol{A}_e T}$.

Data	n	1-norm	2-norm	infinite-norm
Reference data	400	410%/406%	462%/456%	412%/407%
	1000	10.7%/12.5%	8.81%/10.4%	10.5%/12.3%
	4000	1.75%/3.73%	1.61%/3.58%	1.68%/3.59%
	8000	0.989%/2.97%	0.955%/2.93%	0.947%/2.85%
	10,000	0.895%/2.88%	0.875%/2.85%	0.857%/2.79%
	20,000	0.769%/2.74%	0.769%/2.74%	0.744%/2.65%
	40,000	0.738%/2.71%	0.742%/2.71%	0.723%/2.62%
	80,000	0.730%/2.70%	0.736%/2.70%	0.718%/2.61%
Variation data	400	358%/337%	395%/372%	358%/340%
	1000	8.29%/13.7%	6.73%/11.7%	8.31%/13.7%
	4000	3.13%/10.5%	2.97%/10.3%	3.06%/10.2%
	8000	2.59%/10.1%	2.55%/10.0%	2.53%/9.82%
	10,000	2.52%/10.0%	2.50%/10.0%	2.47%/9.77%
	20,000	2.44%/9.95%	2.43%/9.96%	2.38%/9.70%
	40,000	2.41%/9.93%	2.42%/9.95%	2.36%/9.68%
	80,000	2.41%/9.92%	2.41%/9.94%	2.36%/9.68%

Table 5
The relative error in spectral radius between matrixes M and $e^{A_e T}$

n	Reference data		Variation data	
	Triangular-wave pulse	Rectangular-wave pulse	Triangular-wave pulse	Rectangular-wave pulse
400	3.48%	5.07%	400	3.48%
1000	1.33%	2.43%	1000	1.33%
4000	1.10%	2.17%	4000	1.10%
8000	1.09%	2.16%	8000	1.09%
10,000	1.09%	2.16%	10,000	1.09%
20,000	1.09%	2.15%	20,000	1.09%
40,000	1.09%	2.15%	40,000	1.09%
80,000	1.09%	2.15%	80,000	1.09%

5. Conclusion

The stability of the IPS with pulse load involves two aspects. The first aspect is about the periodic steady state of the state variables of the system under the action of the pulse load. The problem refers to the stability of the periodic orbit. The second is about whether there is an unacceptable oscillation, increase or decrease in the system state variable during a pulse period. The problem cannot be explained in terms of the stability of the equilibrium point, so it needs to be further studied. The study on the first aspect will lay the foundation for the study on the second aspect. This paper presents a mathematical model of the IPS with pulse load, deals with the periodic orbit and its Jacobian matrix of Poincaré mapping according to the sensitivity of the state variable at the final moment to that at the initial moment so as to calculate the system stable margin. Also, a state-space averaging model of the system is derived. The state-space averaging method is considered to be approximate to the periodic-orbit method in use in view of a small disturbance in the state variable under the condition of small-signal disturbance. Therefore, the state-space averaging method can be used to analyze the stability of the IPS with pluse load.

References

[1] Steurer M, Andrus M, Langston J, et al. Investigating the impact of pulsed power charging demands on shipboard power quality. Electric ship technologies symposium, 2007. ESTS '07. IEEE. IEEE; 2007. p. 315–21.
[2] Kulkarni S, Santoso S. Estimating transient response of simple AC and DC shipboard power systems to pulse load operations. 2009 IEEE electric ship technologies symposium, Baltimore, MD. 2009. p. 73–8.
[3] Scuiller F. Simulation of an energy storage system to compensate pulsed loads on shipboard electric power system. Electric ship technologies symposium. IEEE; 2011. p. 396–401.
[4] Kulkarni S, Santoso S. Impact of pulse loads on electric ship power system: With and without flywheel energy storage systems. 2009 IEEE Electric Ship Technologies Symposium, Baltimore, MD. 2009. p. 568–73.
[5] Benatmane M, Maltby R. Integrated electric power and propulsion system on land an overview. 2007 IEEE electric ship technologies symposium, Arlington, VA. 2007. p. 7–13.
[6] Ma W. A survey of the second-generation vessel integrated power system. The international conference on advanced power system automation and protection, Beijing, China. 2011.
[7] Doerry N, Mccoy K. Next Generation integrated power system (NGIPS) technology development roadmap. DC, Washington Navy Yard: Naval Sea Systems Command; 2007.
[8] Ebrahimi H, El-Kishky H, Biswass M, et al. Impact of pulsed power loads on advanced aircraft electric power systems with hybrid APU. IEEE international power modulator and high voltage conference (IPMHVC) San Francisco, CA. 2016. p. 434–7.
[9] Salehi V, Mirafzal B, Mohammed O. Pulse-load effects on ship power system stability. IECON 2010 - 36th annual conference on IEEE industrial electronics society, Glendale, AZ. 2010. p. 3353–8.
[10] Kundur Prabha. Power system stability and control. McGraw-Hill Companies; 1994.
[11] Banerjee S, George CV. Nonlinear phenomena in power electronics 2001;vol. 4:59–67. 165-169.
[12] Clark Robinson R. An introduction to dynamical systems: continuous and discrete. New Jersey: Prentice Hall; 2004. pp. 183–187,202–218, 252–258.
[13] Middlebrook R, Cuk S. A general unified approach to modelling switching-converter power stages. 1976 IEEE power electronics specialists conference, Cleveland, OH. 1976. p. 18–34.
[14] Brand L, Bass RM. Extension of averaging theory for power electronics systems. IEEE Trans Power Electron 1996;11(4):542–53.
[15] Bartelt Roman, Oettmeier Martin, Heising Carsten, et al. Scenario-based stability-assessment of converter-fed DC-ship grids loaded with pulsed power. 2011 IEEE electric ship technologies symposium, Alexandria, VA. 2011. p. 468–71.
[16] Weaver WW, Robinett RD, Wilson DG, Matthews RC. Metastability of pulse power loads using the hamiltonian surface shaping method. IEEE Trans Energy Convers 2017;32(2):820–8.
[17] Wang G, Xiao R, Wu X. Analysis of integrated power system with pulse load by periodic orbit. IEEE Trans Plasma Sci 2019;47(2):1345–51.
[18] Woodruff SL, Qi Li, Sloderbeck MJ. Hardware-in-the-loop experiments on the use of propulsion motors to reduce pulse-load system disturbances. 2007 IEEE electric ship technologies symposium, Arlington, VA. 2007. pp. 1-1.
[19] He-feng L, Jun L, Zhihao Y, Feng Z. Optimized operation mode of coordination between the flywheel energy storage and generators for pulsed loads in micro-grid. 2017 2nd international conference on power and renewable energy (ICPRE), Chengdu. 2017. p. 732–6.

Gang Wang was born in Hegang, China. He received the Ph.D. degree in electrical engineering from Tsinghua University, Beijing, China, in 2008. He is currently a Professor and a Doctoral Tutor with the National Key Laboratory of Science and Technology on Vessel Integrated Power System, Navy University of Engineering, Wuhan, China. His research interest is analysis and control of integrated power system.

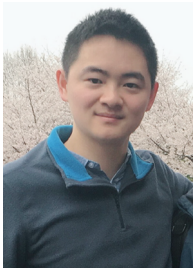

Runlong Xiao was born in Yiyang, China. He received the B.S. degree in electrical engineering and automation from Hunan University, Changsha, China, in 2015, and the M.S. degree with the National Key Laboratory of Science and Technology on Vessel Integrated Power System, Navy University of Engineering, in 2017, Wuhan, China. where he is currently pursuing the Ph.D. degree. His current research interest is Power System Analysis, he is the corresponding author of this paper.

Chen Xu was born in Weihai, China. She received the B.S. degree in automation from Xi'an University of Technology, Xi'an, China, in 2017. She is currently pursuing the M.S. degree with the National Key Laboratory of Science and Technology on Vessel Integrated Power System, Navy University of Engineering, Wuhan. Her current research interest is Power System Analysis.